

# First Measurement of Proton-Proton Elastic Scattering at RHIC

S. Bültmann, I. H. Chiang, R. E. Chrien, A. Drees, R. L. Gill, W. Guryn,  
D. Lynn, C. Pearson, P. Pile, A. Rusek, M. Sakitt, and S. Tepikian  
*Brookhaven National Laboratory, Upton, NY 11973, USA*

J. Chwastowski and B. Pawlik  
*Institute of Nuclear Physics, Cracow, Poland*

M. Haguenauer  
*Ecole Polytechnique, 91128 Palaiseau Cedex, France*

A. A. Bogdanov, S. B. Nurushev, M. F. Runtzo, and M. N. Strikhanov  
*Moscow Engineering Physics Institute, Moscow, Russia*

I. G. Alekseev, V. P. Kanavets, L. I. Koroleva, B. V. Morozov, and D. N. Svirida  
*Institute for Theoretical and Experimental Physics, Moscow, Russia*

M. Rijssenbeek, C. Tang, and S. Yeung  
*Stony Brook University, Stony Brook, NY 11794, USA*

K. De, N. Guler, J. Li, and N. Ozturk  
*University of Texas at Arlington, Arlington, TX 76019, USA*

A. Sandacz  
*Institute for Nuclear Studies, Warsaw, Poland*

(Dated: November 6, 2018)

## Abstract

The first result of the pp2pp experiment at RHIC on elastic scattering of polarized protons at  $\sqrt{s} = 200$  GeV is reported here. The exponential slope parameter  $b$  of the diffractive peak of the elastic cross section in the  $t$  range  $0.010 \leq |t| \leq 0.019$  (GeV/c) $^2$  was measured to be  $b = 16.3 \pm 1.6$  (stat.)  $\pm 0.9$  (syst.) (GeV/c) $^{-2}$ .

PACS numbers: 13.75Cs, 29.27Hj, 14.20Dh

Although elastic scattering has been measured in  $p\bar{p}$  collisions up to  $\sqrt{s} = 1.8$  TeV, the highest energy  $pp$  data reach only to 63 GeV. We present here the first measurement of the slope parameter  $b$  in forward proton-proton elastic scattering obtained by the pp2pp experiment at the Relativistic Heavy Ion Collider (RHIC) at  $\sqrt{s} = 200$  GeV.

The pp2pp experiment [1] is designed to measure polarized  $pp$  elastic scattering at RHIC, which will provide proton beams with polarizations of 0.7 and luminosities up to  $2 \times 10^{32} \text{ cm}^{-2}\text{sec}^{-1}$ . The main goal of the experiment is to study the spin dependence of elastic scattering in the squared four-momentum transfer range  $4 \times 10^{-4} \leq |t| \leq 1.3 \text{ (GeV/c)}^2$  and  $50 \leq \sqrt{s} \leq 500$  GeV.

By measuring elastic scattering of polarized protons in the nonperturbative regime of QCD at RHIC, one has a unique opportunity to probe the spin structure of the nucleon and of the exchanged mediators of the force, the Pomeron and its odd C-parity partner, the Odderon. The pp2pp experiment, part of the RHIC spin program, studies the physics of elastic scattering and diffractive dissociation. It addresses the main unsolved problems in particle physics— long range QCD and confinement.

The slope  $b$  for  $|t| \leq 0.5 \text{ (GeV/c)}^2$  is inherently sensitive to the exchange process, and its dependence on  $\sqrt{s}$  will allow to distinguish among various QCD based models of hadronic interactions. Some interesting features of  $b$  observed in  $p\bar{p}$  are not yet confirmed in  $pp$  elastic scattering. In general, the forward peak does not show a simple exponential behavior. The  $t$  distribution becomes less steep as  $|t|$  increases from  $0.02 \text{ (GeV/c)}^2$  to  $0.20 \text{ (GeV/c)}^2$ , although at the highest Tevatron energies this was not observed. It is therefore of interest to see the  $b$  behavior in the RHIC energy range.

In RHIC the two protons collide at the interaction point (IP), and since the scattering angles are small, scattered protons stay within the beam pipe of the accelerator. They follow trajectories determined by the accelerator magnets until they reach the detectors, which measure the  $x, y$  coordinates in the plane perpendicular to the beam axis. The coordinates are related by the beam transport equations to the corresponding quantities at the IP:

$$\begin{aligned} x &= a_{11} \cdot x_0 + L_{eff}^x \cdot \theta_x^* + a_{13} \cdot y_0 + a_{14} \cdot \theta_y^* \\ y &= a_{31} \cdot x_0 + a_{32} \cdot \theta_x^* + a_{33} \cdot y_0 + L_{eff}^y \cdot \theta_y^* \end{aligned} \quad (1)$$

where  $x_0, y_0$  and  $\theta_x^*, \theta_y^*$  are the positions and scattering angles at the IP and  $a_{ij}$  and  $L_{eff}$  are the elements of the transport matrix. The optimum condition for the experiment is

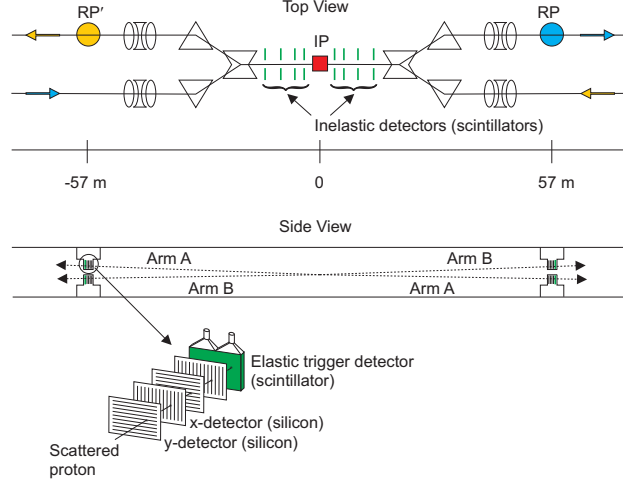


FIG. 1: Layout of the pp2pp experiment. Note the detector pairs RP and RP' lie in different RHIC rings. Scattering is detected in either one of two arms: Arm A is formed from the upper half of RP' and the lower half of RP. Conversely, Arm B is formed from the lower half of RP' and the upper half of RP.

to minimize the dependence of the measured coordinates on the unknown collision vertex, i. e. to have the  $a_{ij}$ 's small and the  $L_{eff}$ 's as large as possible. In that case, called “parallel to point focusing”, rays that are parallel to each other at the interaction point are focused nearly to a single point at the detector. Since in practice such a condition is achieved for one coordinate only, in our case  $y$ , Eq. (1) then simplifies to  $y \approx L_{eff}^y \cdot \theta_y^*$ .

The momentum-transfer interval for the data presented here is  $0.004 \leq |t| \leq 0.032$  (GeV/c)<sup>2</sup>. In our 14 hour run of January 2002, the RHIC orbit betatron function [2] at the IP was  $\beta^* = 10$  m, resulting in  $L_{eff}^y \approx 24$  m. At larger momentum transfers the acceptance is limited by the aperture of the RHIC focusing quadrupoles.

The layout of the experiment is shown in Fig. 1. The identification of elastic events is based on the collinearity criterion, hence it requires the simultaneous detection of the scattered protons in the pair of Roman Pot (RP) detectors [3], RP and RP', on either side of the IP. Additionally, a set of scintillators located outside of the beam pipe near the IP provide detection of inelastic events.

The RP's are insertion devices allowing four silicon strip detectors (SSD) to be positioned just above and below the beam orbits. The SSD's inside the pots record the  $x, y$  coordinates

of the scattered protons. The silicon detectors are made of 0.40 mm thick n-type silicon with  $p^+$ -type implanted strips of 0.07 mm width and a strip pitch of 0.10 mm. Two of the detectors have 512 strips implanted along the longer side of the rectangle, the other two 768 strips perpendicular, resulting in an active area of  $75 \times 45 \text{ mm}^2$ . Each strip is capacitively coupled to an input channel of a SVXIIe [4], which has 128 channels with preamplification, a 32 event pipeline, and a Wilkinson-type ADC.

The amount of charge collected due to a 100 GeV/c proton passing through the silicon detector corresponds to an energy deposit of about 200 keV. In 80% of the events, this deposited energy is confined to a single strip, and otherwise shared between neighboring strips if the particle passed through a  $30 \mu\text{m}$  wide region in between the strips.

The elastic trigger scintillators were 8 mm thick,  $80 \times 50 \text{ mm}^2$  in area, and were viewed by two photomultiplier tubes. To produce a highly efficient and uniform trigger the two signals from the tubes formed a logical OR. The elastic event trigger is a coincidence between signals in the RP's scintillators, belonging either to arm A or arm B (see Fig. 1). The trigger efficiency was greater than 0.99. For each event, time and amplitude were digitized and recorded.

The coordinate in the SSD is calculated as an energy-weighted average of the positions of the hit strips. Clusters of more than three hit strips were excluded. The detection efficiency for every SSD strip was calculated using the redundancy of the silicon planes for identification of elastic events. The average silicon detector plane efficiency for arm A was 0.97.

The collinearity of elastic events implies that the two coordinates obtained from the silicon detectors on either side of the interaction point are correlated. This correlation is shown for the  $y$  coordinates from arm A in Fig. 2. The widths of the coordinate difference distributions,  $\sigma_x$  and  $\sigma_y$ , were determined. Events for which  $\sqrt{\Delta x^2 + \Delta y^2} \leq 4 \sqrt{\sigma_x^2 + \sigma_y^2}$  were retained for the analysis. The widths are dominated by the beam angular emittance of about  $12\pi \mu\text{m}$  and by the uncertainty of about 60 cm (rms) in the vertex position along the beam axis.

At least six of the possible eight planes were required to have hits to be accepted for elastic events. Out of 196,000 elastic triggers for arm A about 84% were reconstructed. Most reconstruction failures are accounted for by the larger area of the scintillator compared to the active area of the SSD packages. The above mentioned correlation cut of  $4\sigma$  removed

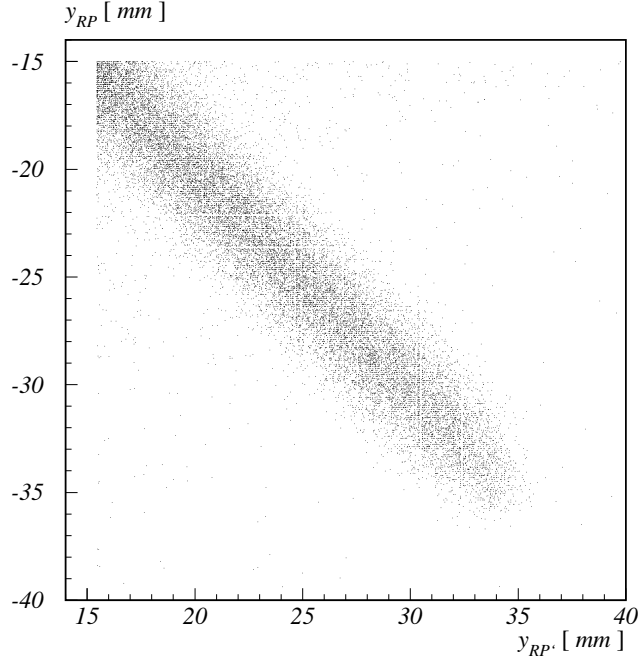


FIG. 2: Correlation between the  $y$  coordinates as measured by the two detectors of arm A for elastic events before cuts being applied.

another 3.8%, while the requirement of six hit planes contributing to the track reconstruction cut another 0.3%. To reduce the contamination of the elastic event sample with tracks from background particles, not more than two planes with more than one hit per event were accepted. This reduced the event sample by another 3.2%, giving a total of 153,000 elastic events for this arm. A similar analysis was carried out for arm B, but because of the noise level being considerably higher, it was used only for consistency checks, but not included in the final analysis presented here.

For each event the scattering angle  $\theta$  and azimuth  $\phi$  were calculated for each proton and then averaged. The scattering angle is related to the square of the four-momentum transfer,  $t$ , via  $-t \approx (p \cdot \theta)^2$ . A restriction of the  $\phi$  range leads to a uniform geometric acceptance in a limited  $t$ -range. For  $45^\circ < \phi < 135^\circ$  or  $225^\circ < \phi < 315^\circ$  that range is  $0.010 \leq |t| \leq 0.019$  (GeV/c)<sup>2</sup>. In Fig. 3 the correlation between  $t$  and  $\phi$  is shown for reconstructed events. The determination of the slope parameter  $b$  is confined to the  $t$  region for which no acceptance correction is required. The final selection therefore yields 58,511 events. The uncorrected  $dN/dt$  distribution resulting from the  $\phi$ -cut is shown in Fig. 4 together with the acceptance function obtained from Monte Carlo studies.

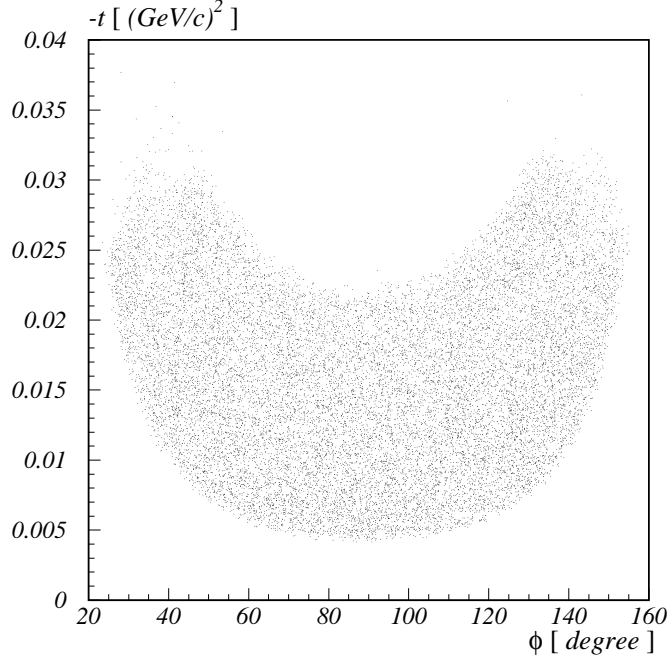


FIG. 3: Correlation between  $t$  and  $\phi$  for reconstructed events.

The differential cross section  $d\sigma/dt$  for elastic scattering in the forward angle region is determined by Coulomb and nuclear amplitudes and the interference term between them. The cross section is given by (see for example Ref. [5])

$$\begin{aligned} \frac{d\sigma}{dt} = & 4\pi (\hbar c)^2 \left( \frac{\alpha G_E^2}{t} \right)^2 \\ & + \frac{1 + \rho^2}{16\pi (\hbar c)^2} \cdot \sigma_{tot}^2 \cdot e^{-b|t|} \\ & - (\rho + \Delta\Phi) \cdot \frac{\alpha G_E^2}{|t|} \cdot \sigma_{tot} \cdot e^{-\frac{1}{2}b|t|}, \end{aligned} \quad (2)$$

with  $\alpha$  the fine structure constant,  $G_E$  the electric form factor of the proton,  $\Delta\Phi$  the Coulomb phase[6],  $\rho$  the ratio of the real to imaginary part of the forward scattering amplitude,  $\sigma_{tot}$  the total cross section, and  $b$  the nuclear slope parameter. The dominant contribution in our  $t$  region is the second term in this expression.

A least squares fit was performed to the distribution of Fig. 4 using Eq. (2) with  $b$  and a normalization constant as free parameters. The total cross section and  $\rho$  were fixed to  $\sigma_{tot} = 51.6$  mb [7] and  $\rho = 0.13$  [8]. These values of  $\sigma_{tot}$  and  $\rho$  come from fits to the existing  $pp$  data taken at energies below 63 GeV and world  $p\bar{p}$  data.

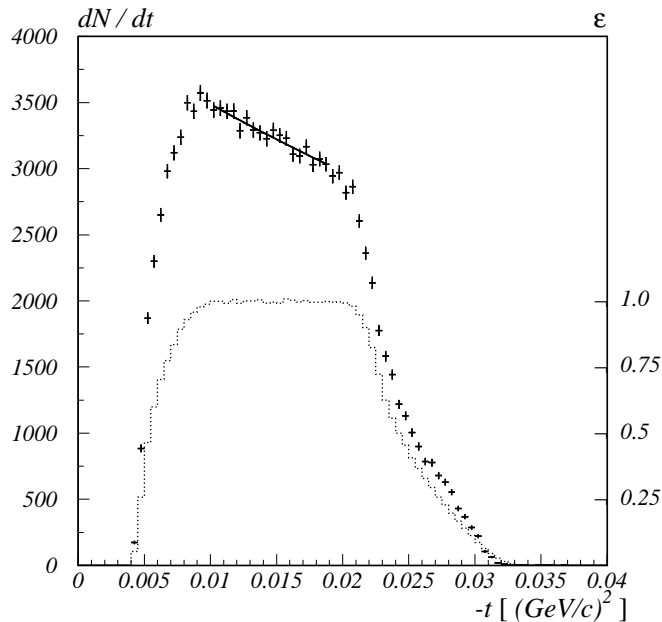


FIG. 4: The distribution of  $dN/dt$  within the  $\phi$  region selected as described in the text. The two distributions shown are the measured data and the simulated acceptance function. The fit is shown by the solid line.

The resulting slope parameter is

$$b = 16.3 \pm 1.6 \text{ (stat.)} \pm 0.9 \text{ (syst.) (GeV/c)}^{-2}.$$

The evaluation of the systematic errors due to the uncertainty in beam emittance, vertex positions and spread, beam transport matrix elements, and incoming beam angles was based on Monte Carlo simulations. These simulations used the geometry of the experimental setup and efficiency of the detectors as an input. The largest single source of the systematic error was the uncertainty of the initial colliding beam angles.

There is also a correlation between  $b$  and the values of  $\rho$  and  $\sigma_{tot}$ . We find that the changes  $\Delta\rho = \pm 0.02$  and  $\Delta\sigma = \pm 4$  mb result in changes in  $b$  of  $\Delta b = \mp 0.32 \text{ (GeV/c)}^{-2}$  and  $\Delta b = \mp 0.07 \text{ (GeV/c)}^{-2}$ , respectively.

An independent analysis of the data was performed using different selections of hits and elastic events. In particular, a  $t$ -dependent cut on  $\phi$  was applied, which allowed an increase in the  $t$  range and the number of accepted elastic events. The  $b$  slope values obtained from both analyses agree within statistical errors.

Our result for the slope parameter  $b$  is shown in Fig. 5 together with the world data on



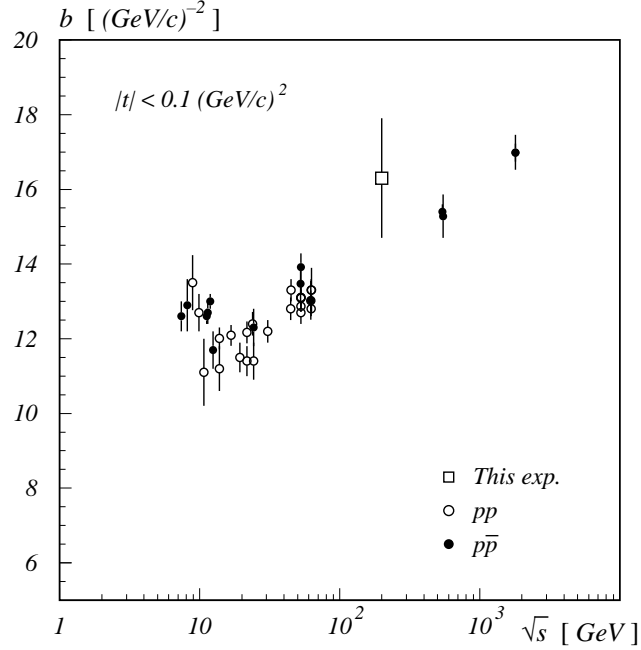


FIG. 5: The result for the slope parameter  $b$  of this experiment compared to the world  $pp$  and  $p\bar{p}$  data set. The data are drawn from the Durham Database Group (UK). Only statistical errors are shown.

elastic  $pp$  and  $p\bar{p}$  scattering. This result is about one standard deviation higher than an extrapolation of world data to the energy of this experiment [7], [9], [10].

In the future, a full complement of two sets of Roman Pot detector pairs will be used, two pairs at each side of the IP, to allow a direct measurement of the scattering angles. This will reduce the systematic error due to the uncertainty of the vertex position. An expected increase of the RHIC luminosity will result in a reduction of the statistical error and will make the studies of the polarized observables  $A_N$  and  $A_{NN}$  feasible.

The research reported here has been performed in part under the US DOE contract DE-AC02-98CH10886, and was supported by the US National Science Foundation and the Polish Academy of Sciences. The authors are grateful for the help of N. Akchurin, D. Alburger, Y. Onel, A. Penzo, and P. Schiavon at an early stage of the experimental design and the support of the BNL Physics Department, Instrumentation Division, and C-A Department at the RHIC-AGS facility.

- 
- [1] W. Guryn *et al.*, RHIC Proposal R7 (1994) (unpublished); V. Kanavets, Czech. J. Phys., Suppl. A, **53**, A21 (2003)
  - [2] M. A. Harrison, The RHIC Project, Fifth European Particle Accelerator Conference, Geneva (1996)
  - [3] R. Battiston *et al.*, Nucl. Instr. Meth. **A238**, 35 (1985)
  - [4] R. Lipton, Nucl. Instr. Meth. **A418**, 85 (1998)
  - [5] U. Amaldi *et al.*, Phys. Lett. **B43**, 231 (1973)
  - [6] B. Z. Kopeliovich and A. V. Tarasov, Phys. Lett. **B 497**, 44 (2001).
  - [7] A. Donnachie and P. V. Landshoff, Phys. Lett. **B296**, 227 (1992)
  - [8] C. Augier *et al.*, Phys. Lett. **B315**, 503 (1993)
  - [9] Martin M. Block, Nuc. Phys **B** (Proc. Suppl.) **71** 378 (1999)
  - [10] B. Z. Kopeliovich, I. K. Potashnikova, B. Povh, and E. Pedrazzi, Phys. Rev. **D63** 054001 (2001)